THE JOURNAL OF PHYSICAL CHEMISTRY C

ARTICLE

pubs.acs.org/JPCC

Tryptophan−Gold Nanoparticle Interaction: A First-Principles Quantum Mechanical Study

Prachi Joshi,[*,†,§] Vasundhara Shewale,[†] and Ravindra Pandey[*,†]

[†]Department of Physics, Michigan Technological University, Houghton, Michigan 49931, United States

Virendra Shanker[§]

[§]National Physical Laboratory (CSIR), Dr. K. S. Krishnan Marg, New Delhi-110012

Saber Hussain[‡]

[‡]US Air Force Research Laboratory/HEPB, Wright Patterson Air Force Base, Dayton, Ohio 45433-5707, United States

Shashi P. Karna[⊥]

[⊥]US Army Research Laboratory, Weapons and Materials Research Directorate, ATTN: RDRL-WM, Aberdeen Proving Ground, Maryland 21005-5069, United States

ABSTRACT: The nature of interaction between tryptophan (Trp) and gold (Au) nanoparticles is studied using first-principles density functional theory calculations and described in terms of equilibrium configurations, interaction energies, density of states, molecular orbitals, and charge density. The calculated results find the binding involving both carboxyl and indole functional groups with mixed salt−bridge and charge−solvation structure to be energetically preferred and is attributed to the stronger-than-expected π interactions facilitated by the indole group in Trp. In the Trp−Au conjugates, modification of the molecular orbitals associated with Trp occurs because states associated with Au and the hybrid orbitals have mixed metal−molecule character. We find that the nonradiative energy transfer from excited states of Trp to hybrid states of Trp−Au may reduce intrinsic fluorescence intensity of Trp in the conjugated system.

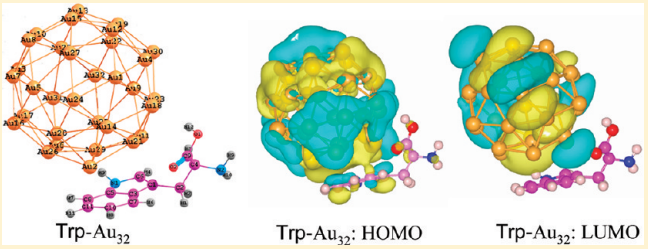

1. INTRODUCTION

The miniaturization of structures in the guise of nanoscale materials has created a so-called nanoplatform for applied biomedical research in developing novel and improved diagnostics and therapeutics.[1] Nanoparticles offer large surfaces for reactions involving biomolecules, thus providing a promising pathway to combine biomolecular functionality with unique electronic and optical attributes of nanoparticles for creation of hybrid nanoscaffolds. Such scaffolds with specific features are of particular interest in recognition and modulation of biomacromolecules, protein interactions, protein−nucleic acid interactions, enzyme activity, biomimetic reactions, etc.[1−3] Because of intriguing optoelectronic properties and biocompatibility, gold nanoparticles have widely been exploited for diagnostics and therapeutic applications.[2] The long-term fascination for gold was substantially facilitated by the ease of their size-controlled synthesis and functionalization with multifunctional ligands such as amino acids, proteins, peptides, and DNA.[2] It was previously established that serum proteins become associated with nanoparticles in biological medium and form protein 'corona', which defines the biological identity of the particles within the biological system thus making protein−nanoparticle interaction of particular interest.[4] The underlying fact is that the adsorption of proteins on nanoparticles can alter their three-dimensional structure, activity, and biological responses that can lead to unpredicted perturbations in the biosystem.

Protein−nanoparticle interactions and their effect on protein structure and activity are generally determined by various spectroscopic and thermodynamic methods. For example, intrinsic fluorescence quenching is a powerful spectroscopic tool for investigating protein structure and binding upon interaction with nanoparticles.[5,6] The fluorescence of proteins is due to aromatic amino acid residues, among which tryptophan (Trp) has the stronger fluorescence and higher quantum yield attributed to the $\pi-\pi^*$ transitions of the indole functional group.[7,8] Trp is an essential amino acid of the human diet and is known to

Received: July 23, 2011
Revised: October 8, 2011
Published: October 16, 2011

dx.doi.org/10.1021/jp2070437 | J. Phys. Chem. C 2011, 115, 22818–22826

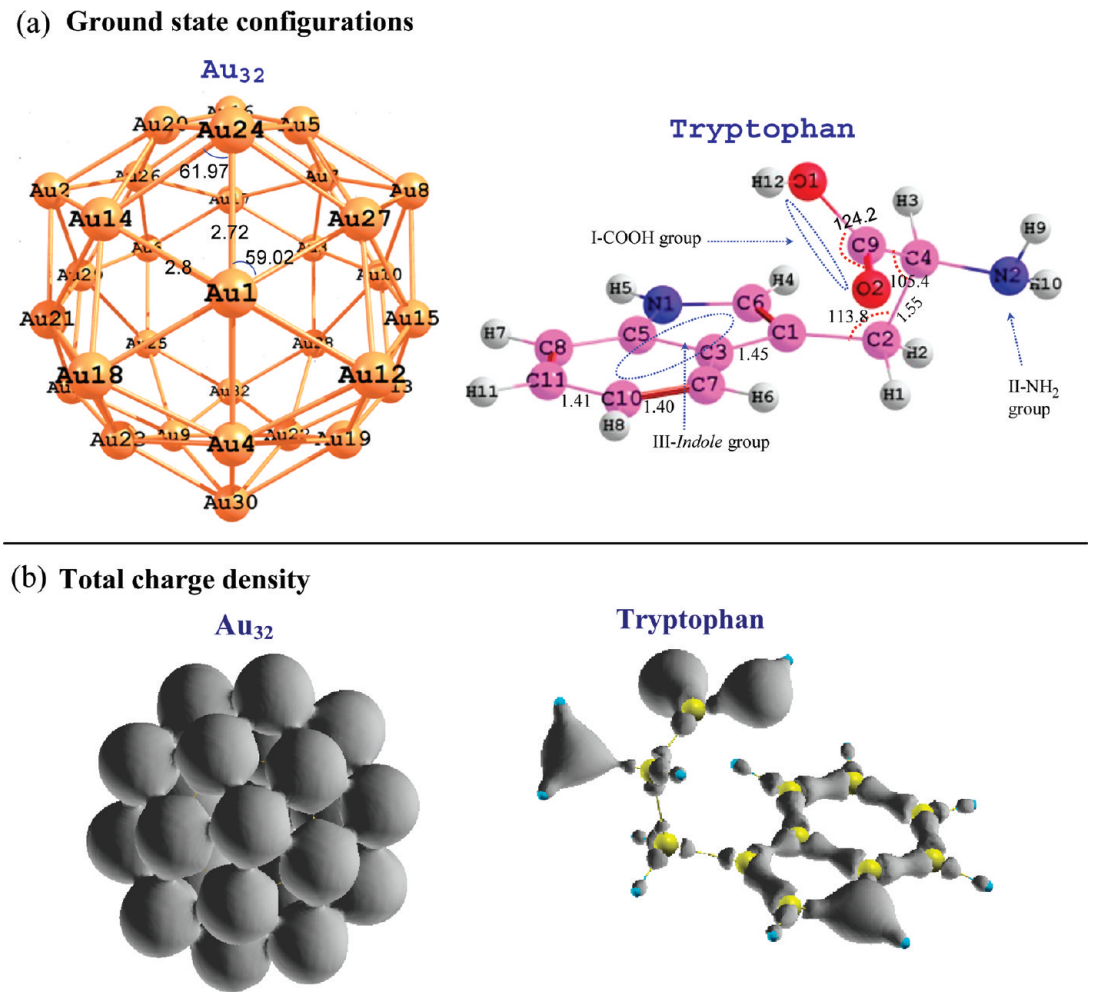

Figure 1. The calculated ground-state configurations and total charge density of (a) the gold nanocluster (Au_{32}) and (b) tryptophan (Trp). The Au_{32} interaction sites of tryptophan are also shown. Charge density is shown at one-third of its maximum isosurface value.

form hydrogen bonds together with weak ionic bonds in a conjugated system. Also, the indole group contains a benzene ring fused with a nitrogen-containing pyrrole ring, thus a delocalized π electron cloud to interact. At the excitation wavelength of 280 nm, the fluorescence of proteins is dominated by Trp along with minor contributions from tyrosine and phenylalanine. The intensity and wavelength of Trp fluorescence are sensitive to the environment and hence indicative of the protein conformational alterations upon binding to nanoparticles.

Earlier studies suggested that gold efficiently quenches the fluorescence of Trp,[9] and efficiency of quenching determines the binding affinity and accessibility of gold particles to the Trp residue in proteins. In the experimental study of bioconjugated gold nanoparticles with BSA protein, the static mode of intrinsic Trp fluorescence quenching revealed ground-state complexation between protein and nanoparticles.[5,10,11] The moderate binding observed for gold−BSA conjugation was consistent with weak van der Waals and hydrophobic interactions between nanoparticle and biomolecules.[5,10,11] Also, in recent studies, Trp- and Trp-based peptides were used for synthesizing stable Au nanoparticles in water.[12,13] The study on Trp-reduced Au nanoparticles suggested indonyl polymerization at the Au surface.[12] We now investigate the Trp fluorescence quenching by gold nanoparticles and their binding interaction using quantum mechanical methods, though it has been largely investigated experimentally.

We employed first-principles methods based on density functional theory (DFT) to determine the details of the interaction between gold (Au) nanoparticles and the amino acid tryptophan (Trp). We will determine the (i) preferred interaction site of Trp, (ii) chemical bonding in Au−Trp bioconjugates, and (iii) modifications to Trp electronic states that may be responsible for its fluorescence quenching in the bioconjugate configuration.

Researchers have shown keen interest in searching for stable clusters as building blocks of nanostructured materials. The highly symmetric small clusters of cagelike structures exhibiting exceptional stability and reactivity are considered promising candidates especially since the discovery of C_{60}, C_{70}, and C_{20} cagelike clusters.[14] A recent report on the magic numbers in gold clusters using the shell jellium model suggests that Au_{32} is highly stable and a potential candidate for studying cagelike structures with an energy gap comparable to other cage structures: C_{60}, Au_{16}, Au_{42}.[15] During an extensive search for electron numbers up to 110, the shell jellium model predicted cagelike structures to appear for electron number 32 or 90 for the clusters.[15] The model explained the stability and exceptional properties of the newly found magic number 32 due to the relativistic effects, high HOMO−LUMO energy gap, and aromaticity of the Au_{32} cage.[15,16]

dx.doi.org/10.1021/jp2070437 |J. Phys. Chem. C 2011, 115, 22818–22826

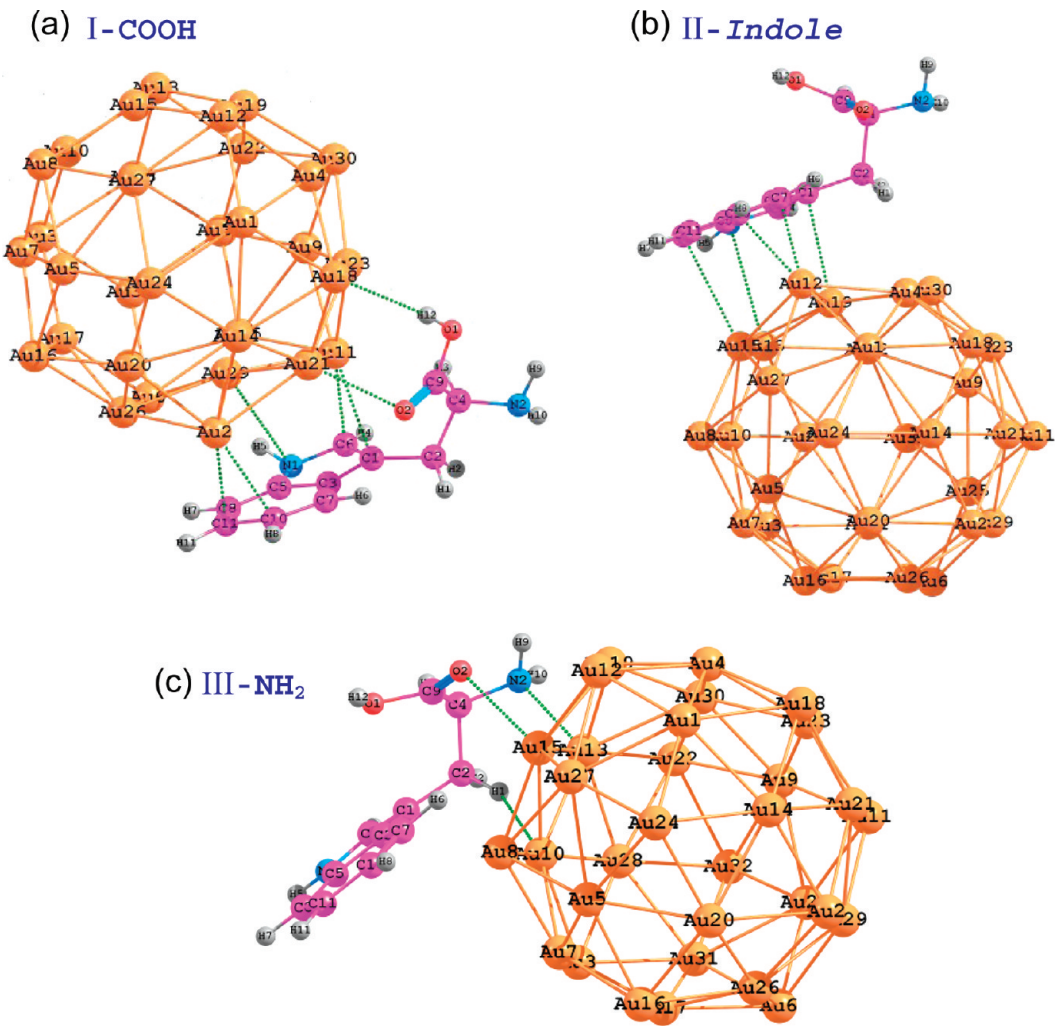

Figure 2. The ground-state configurations of the Trp−Au_{32} conjugate for the different sites of interaction between Trp and Au_{32}.

Therefore, a cagelike hollow gold cluster, Au_{32} of diameter 8.9 Å (∼ 9 Å), was used to study the interaction of Trp with representative gold nanoparticles.

The binding offered by Trp are salt-bridge interaction involving the carboxylic group (COO^-), charge−solvent interaction involving the indole ring, and amine group interaction involving the NH_2 group.[17] Trp is reported to form a very weak zwitterionic state in the gas phase,[18] which is not considered in the present study. The equilibrium configurations with corresponding interaction energies, density of states, molecular orbitals, and charge density distribution of the Trp−Au_{32} complex were obtained through DFT-based quantum mechanical calculations, and results are discussed to elaborate the details of the interaction between Au and Trp.

2. COMPUTATIONAL DETAILS

All calculations were carried out within the framework of density functional theory (DFT) as implemented in SIESTA code using the exchange-correlation function proposed by Perdew, Burke, and Ernzerhof (PBE).[19,20] Only the valence electrons of each chemical species in the Trp and Au nanocluster were treated explicitly, and their interactions with the ionic cores were described by ultrasoft norm-conserving pseudopotentials using the Trouiller and Martins scheme.[21] The valence configurations of H ($1s^1$), C ($2s^2\,2p^2$), N ($2s^2\,2p^3$), O ($2s^2\,2p^4$), and Au ($5d^{10}\,6s^1$) were represented by double-ζ basis sets with polarization functions (DZP).[22] The numerical integrals were performed on a real space grid with an equivalent energy cutoff of 3400 eV. The calculations were considered to be converged when the force on each ion was less than 0.001 eV/Å. Also, total energy convergence criterion of 10^{-5} eV was used.

3. RESULTS AND DISCUSSION

3.1. Au_{32}. The 32 atom cluster of Au was found to favor cagelike structure, hence termed a golden fullerene.[23] The calculated ground-state configuration of Au_{32} has icosahedral I_h symmetry with a hollow cluster shape as shown in Figure 1a. The geometry was obtained by placing one atom on each pentagon of a dodecahedron. The cluster demonstrated only two different kinds of sites on the cage: 12 sites with co-ordination number five and 20 sites with coordination number six, i.e., each atom binds to either five or six neighboring gold atoms. In other words, the symmetry is similar to the truncated icosahedron C_{60}, with interchanged vertices and planes. The bond lengths of 2.72 and 2.8 Å were obtained for five-coordinated sites and six-coordinated sites, respectively (Figure 1a). These values are in

dx.doi.org/10.1021/jp2070437 |J. Phys. Chem. C 2011, 115, 22818–22826

Table 1. Calculated Structural and Electronic Properties of the Isomeric Configurations of the Trp−Au_{32} Conjugate

isomers	I−COOH group	II−indole	III−NH_2
binding energy/eV	−2.72	−1.86	−1.8
$R_{(cluster\text{-}Trp)}$	–	–	–
Au−N	3.0	3.31	2.60
Au−O	2.58	–	2.9
Au−$C_{indole\text{-}benzene}$	2.48	2.35	–
Au−$C_{indole\text{-}pyrrole}$	2.38	2.95	–
Au−H	2.57	2.71	2.40
dipole moment/D	5.97	3.78	7.44
HOMO−LUMO gap/eV	1.2	1.51	1.45
Mulliken charge/e^-	Au = −0.062	Au = −0.08	Au = −0.13
	Trp = +0.062	Trp = +0.08	Trp = +0.13

agreement with the values of 2.74 and 2.85 Å for five- and six-coordinated sites, calculated using density functional theory with generalized gradient approximation in Au_{32}, respectively.[23] The gap between the highest occupied molecular orbital (HOMO) and the lowest unoccupied molecular orbital (LUMO) is calculated to be 1.31 eV. The total charge density of Au_{32} is also shown in Figure 1b.

3.2. Tryptophan. The presence of an indole functional group together with amine and carboxyl functional groups is the discriminating structural characteristic of the aromatic amino acid residue tryptophan (Trp). Figure 1 shows the optimized ground-state configuration and total charge density of the Trp molecule. The indole ring is oriented perpendicular to the carboxyl and amine groups. In the optimized configuration, the indole ring is 113.77° out-of-plane with respect to the plane containing COOH and NH_2 functional groups, i.e., C1−C2−C4. The C−C and C═C bond lengths in the hexagonal benzene ring of indole are 1.42 and 1.40 Å, respectively, whereas the C−C and C═C bond lengths of the pentagonal pyrrole ring of indole are 1.45 and 1.39 Å, respectively. The C−C bond distinguishing a plane of the indole ring and COOH/NH_2 functional groups is 1.56 Å, making an angle (C2−C4−C9) of 105.45° with the COOH group directed toward the indole ring. The O−C−O angle of the COOH group is 123.23°. The calculated HOMO−LUMO gap and dipole moments are 3.66 eV and 4.01 debye (D), respectively. The calculated values of bond lengths and bond angles of Trp corroborates previously reported values obtained at the same level of theory.[24]

3.3. Trp−Au_{32} Conjugates. *3.3.1. Structural Properties.* The optimized isomeric configurations of Trp−Au_{32} conjugates involving (i) COOH (ii) indole, and (iii) NH_2 functional groups as preferred interaction sites are presented in Figure 2. No geometrical constraints were imposed to obtain the optimal structures of these isomeric configurations of Trp−Au_{32}. The binding energy, bond lengths, dipole moment, and HOMO−LUMO energy gap of the optimized isomeric configurations are listed in Table 1.

The binding energy of the Trp−Au_{32} cluster complex is calculated as the difference of the energy associated with the equilibrium configuration and the energies associated with the isolated cluster and Trp. As noted from Table 1, the salt-bridge structure involving the COOH group appears to be energetically more favorable than the two comparably interacting indole and NH_2 groups. The larger binding energy of Trp−Au_{32} in the COOH group conjugation appears to result from interaction of Au with carbonyl oxygen atoms (Figure 2a). Besides O_{Trp}−Au interaction, there exists a weak nonconventional O_{Trp}−H···Au interaction which seems to provide additional stability for the Trp−Au complex. Figure 2a also shows Au atoms interacting with the indonyl functional group including both the pyrrole and benzene ring in Trp. There are some structural changes observed for Trp: Angle C1−C2−C4 is found to be 117° compared to the initial value of 113.77°, and the angle C2−C4−C9 becomes 111.9° compared to its initial value of 105.45°. However, none of the H_{Trp} is found to be perturbed. During indole group interaction, Au atoms are found interact well with the indole group of Trp (Figure 2b). Though no noticeable structural changes occurred during indole group interaction, the angles C1−C2−C4 and C2−C4−C9 show minor alteration and are found to be 114.54° and 106.93°, respectively. Note that, unlike COOH site interaction having an indole contribution, the NH_2 site interacts through the nitrogen of the amine, oxygen of the carboxyl, and hydrogen of the carbon backbone (Figure 2c). Figure 2c shows double coordination of Au with COOH and NH_2 groups, and the angles C1−C2−C4 and C2−C4−C9 are 118.76° and 112.69°, respectively. Additionally, the angle between the COOH group and NH_2 group in Trp is decreased to 106.33° from an initial value of 109.52°.

In protein chemistry, structures involving the COO^- group of an amino acid are known as salt-bridge structures, whereas interactions involving the indole ring are represented in charge-solvent structures.[25] Following this nomenclature, the Trp−Au_{32} isomer formed through COOH group interaction can be classified as a salt-bridge structure, but as noted from Figure 2a and Table 1, the Au cluster interacts equally with the indole group during this interaction. Hence, the isomeric configuration involving the COOH group may be considered to have characteristics of both salt-bridge as well as charge solvation structure, therefore showing maximum binding energy (Table 1). Likewise, the isomeric configuration involving the indole group may be considered as charge solvation structure. The isomer with the NH_2 group shows double coordination with COOH and NH_2 groups (Figure 2c). Thus, the calculated results show ground-state complexation in agreement with the experimental observation[10,11] with a preference for mixed salt-bridge and charge solvation type bonding interaction.

3.3.2. Electronic Structure. The Mulliken charge analysis of the isomeric configurations of the Trp−Au_{32} complex reveals a small charge transfer during conjugation and is noted from Trp to Au cluster in all three sites of interaction. The results therefore excluded charge transfer as the main mechanism for Trp-Au_{32} conjugation for COOH and indole group interaction. However, the charge transfer is comparatively higher in the case of NH_2 group interaction, which may govern the conjugation. This is in agreement with the relatively larger dipole moment, 7.44 debye (D), of the complex compared to the native Trp during NH_2 group interaction, suggesting rearrangement of electron density upon complex formation. The comparatively large dipole moment of the COOH group relative to that of the indole group is correlated with a larger structural rearrangement demonstrated during the formation of COOH group conjugation whereas no such structural perturbation is noted for indole group conjugation. Interestingly, note that both COOH and indole interaction sites, showing nearly the same values of small charge transfer, share a common factor, i.e., indole group, during conjugation with Au_{32} (Figure 2). The relatively stronger-than-expected interactions offered by the indole group, demonstrated by the

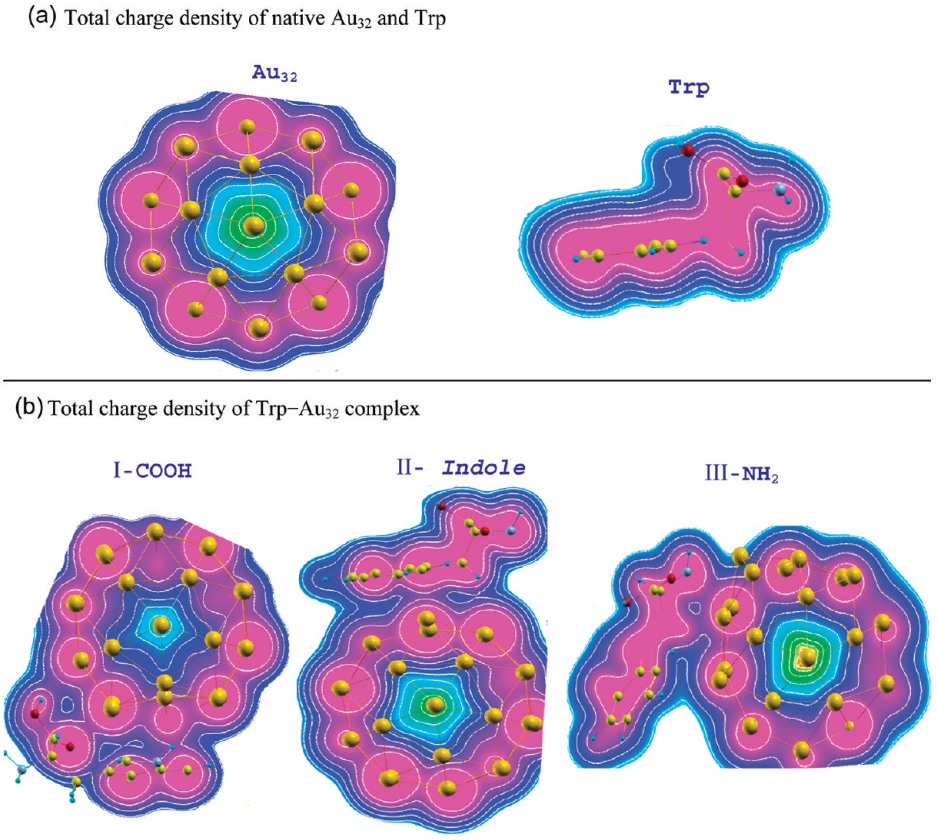

Figure 3. Total charge density plot of Au_{32}, Trp, and isomeric configurations of the Trp−Au_{32} conjugate projected along the (001) plane. A superimposed ball and stick model identifies the atoms in the complex. Total charge density is shown at one-third of its maximum isosurface value.

computed results, basically originate from donation of the π electron cloud to the Au atoms. The planarity of indole also maximizes the delocalization interaction. These effects are realized in the previous studies.[26] Thus, our calculation suggests that the preferred nature of the bonding is dominated by π interactions with a small charge transfer involving the indole functional group. The present study provides evidence verifying the indonyl role in auric chloride reduction.[12,13] It is considered that indole has an inherent ability to interact with Au nanoparticles through delocalized π electrons, and this active indonyl further induces the polycondensation of the π electron cloud for making a long π conjugated system in Trp molecules at the Au surface. In fact, amino acids interact differently with Au nanoparticles. For example L-cysteine undergoes oligomerization, and methionine was found to form a H-bonding network at the Au surface depending upon the active functional groups and reaction conditions.[27,28]

Figure 3 shows the charge density plots projected along the (001) plane for all the isomeric configurations of the Trp−Au_{32} complex (Figure 3b) compared to native Trp and Au_{32} (Figure 3a). Figure 3b clearly shows that the interaction and charge redistribution is taking place through the indole ring and carbonyl oxygen in the Trp−Au_{32} complex for I−COOH group interaction, corroborating the previous results. For the II−indole group complex, the charge density plot in Figure 3b implies indonyl participation during indole group interaction, and weak charge delocalization indicates the existing π electronic interactions for Trp−Au_{32} conjugation. The charge density plot for III−NH_2 in Figure 3b reveals the electronic charge redistribution during NH_2 group interaction, and it is higher than the other two mentioned interactions. Hence, charge density results provide evidence for the nature of interactions as predicted in section 3.3.1 and Figure 2.

Previous experimental studies demonstrated the altered optical absorption characteristics and quenching of fluorescence of Trp upon binding to Au nanoparticles.[12,13,29] In a similar way, the experimental protein−nanoparticle studies described that the binding site of Au nanoparticles in BSA contains Trp in the near vicinity, hence resulting in its fluorescence quenching.[10,11] Because the spectral signatures of the protein−Au conjugate are dominated by the $\pi-\pi^*$ transition of Trp's indole functional group, the formation of the complex could modify the electronic states or introduce new states in Trp, resulting in a loss of fluorescence energy. To examine this, we plot the HOMO and low-lying excited states of pristine Trp, Au_{32}, and Trp−Au_{32} isomers in Figure 4.

As seen from the figure, the HOMO and LUMO in the case of pristine Trp are localized at the indole functional group. However, significant modification to the nature of the molecular orbitals, and hence the charge redistribution, happens upon Trp−Au_{32} conjugate formation. The orbitals associated with Au atoms appear as low-lying LUMO in the energy spectrum of all three isomers. This LUMO may potentially act as an acceptor from the excited fluorescence state of Trp in the complex, thus reducing the fluorescence intensity. The higher LUMOs, i.e., LUMO+1, LUMO+2, are delocalized over the Au atoms as well as on the interacting Trp atoms. The delocalized higher LUMOs indicate that the hybridization in Trp−Au_{32} yields orbitals of

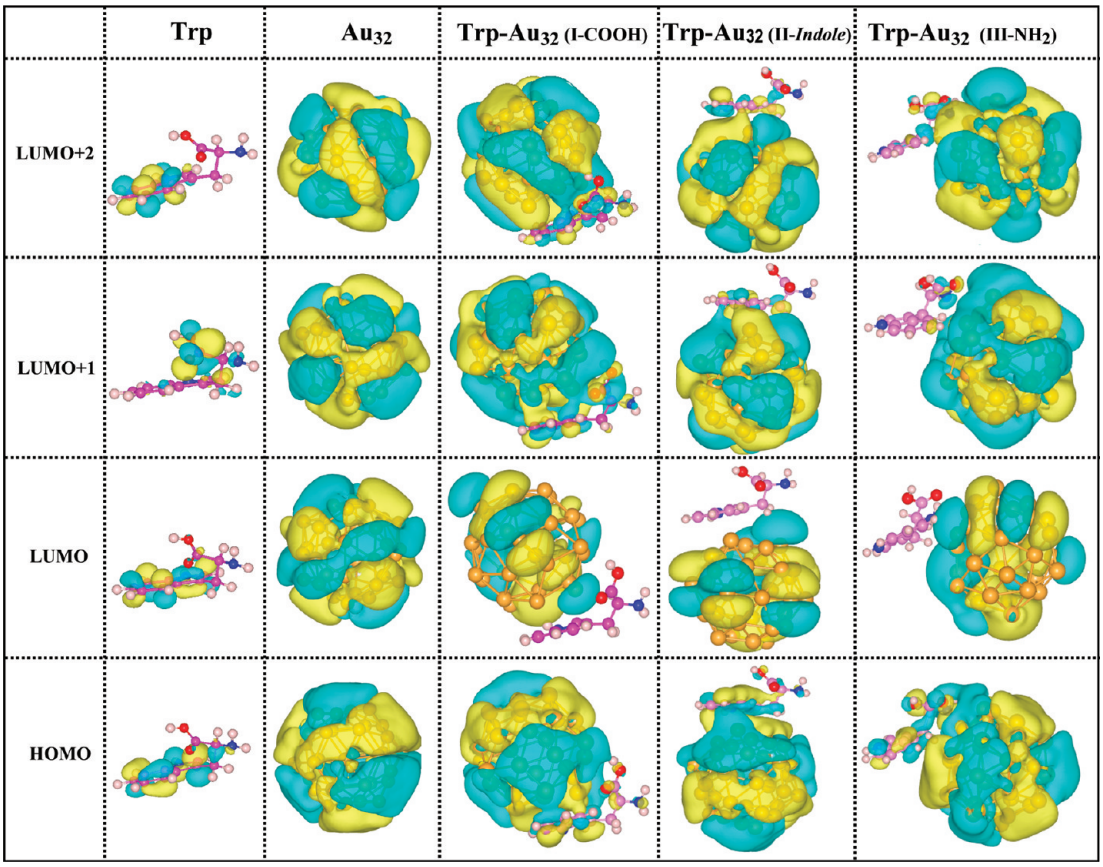

Figure 4. The contour plots of molecular orbitals of pristine Trp, Au_{32}, and Trp−Au_{32} conjugate isomers shown at one-half of its maximum isosurface value.

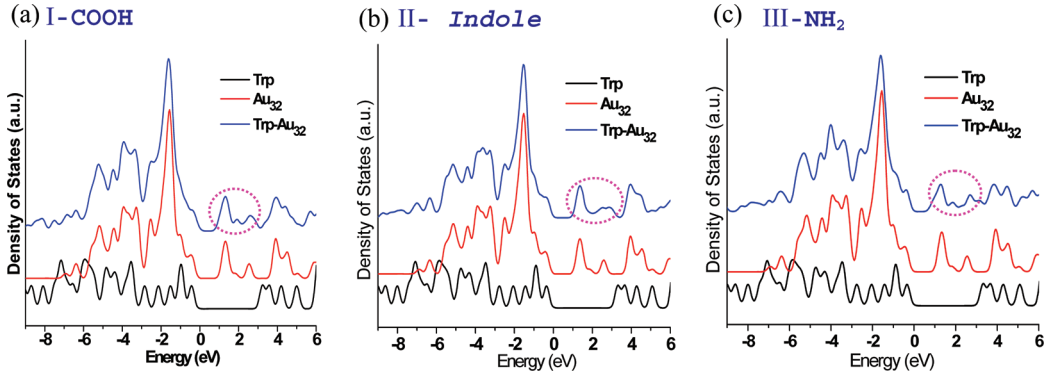

Figure 5. Density of states of Trp, Au_{32} and Trp−Au_{32} conjugate isomers: (a) I−COOH, (b) II−indole, and (c) III−NH_2. The HOMO is aligned to origin in the energy scale. The low-lying hybrid excited states introduced by Au are marked by pink circles.

mixed metal−molecule character. Appearance of Au-localized LUMO, hybrid LUMO+1, and LUMO+2 orbitals is further confirmed by total density of states (DOS) of isomers as shown in Figure 5. The DOS of Trp−Au_{32} isomers show hybrid states near the Fermi energy that is introduced in the system by Au.

Experimental evidence from UV−vis spectroscopy suggests that the absorption wavelength (λ_{max}) for $\pi-\pi^*$ transitions in bare Trp at 270 nm shifted to 260 nm, and in Trp-based peptide the λ_{max} was shifted to 265 nm from the initial value of 280 nm during interaction with Au nanoparticles.[12,13] The appearance of Au-induced hybrid states near the Fermi energy in the present study (Figures 4 and 5) explains the spectral shift observed in the Trp spectrum upon interaction with Au nanoparticles during experiments.

The modification to Trp electronic states has a significant effect on its fluorescence characteristics. Experimental studies have shown that the emission of bare Trp at 353 nm diminished rapidly after addition of Au nanoparticles under excitation at 278 nm.[29] The appearance of Au_{32}-localized LUMO in Trp−Au_{32} explains the mechanism of fluorescence energy transfer from Trp to Au, which is recognized as fluorescence quenching in fluorescence spectroscopy experiments. The detailed process

dx.doi.org/10.1021/jp2070437 |J. Phys. Chem. C 2011, 115, 22818–22826

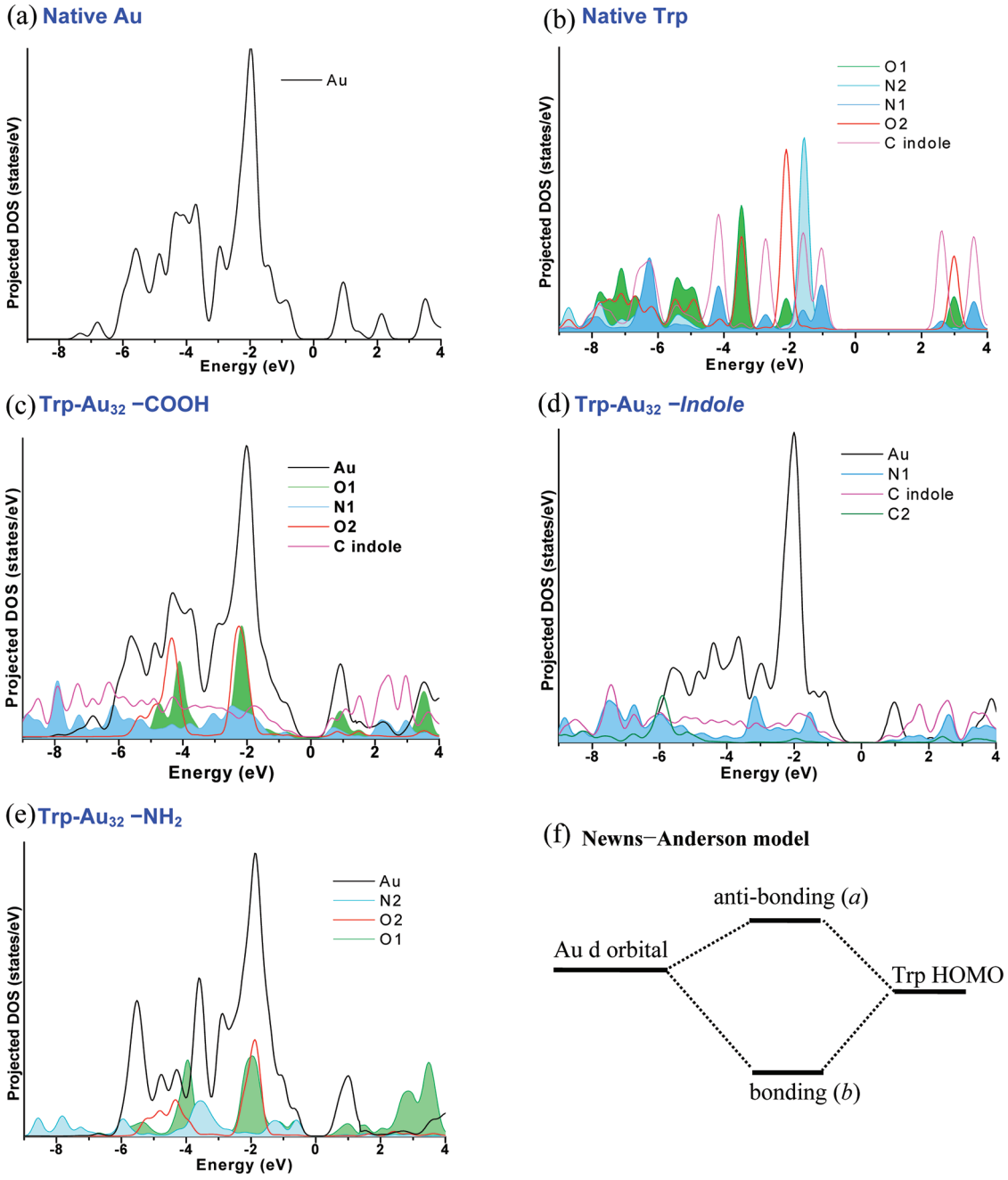

Figure 6. The projected density of states (PDOS) of interacting atoms in (a) native Au_{32}, (b) native Trp, (c) COOH group, (d) indole group, (e) NH_2 group isomers of the Trp−Au_{32} conjugate, and panel f shows the Newns−Anderson bonding scheme. Fermi levels are aligned at the origin of the energy scale.

may be correlated with time-resolved fluorescence decay and lifetime measurements. It is not only Trp that undergoes electronic-state modification; Au also faces the same, as seen in Figures 4 and 5. For example, the surface plasmon of Au undergoes a change upon interaction with Trp. Also, experimentally shown enhanced SERS signals in Trp-conjugated Au nanoparticles is the evidence for modification to the optoelectronic properties of Au.[29] The calculated results in the present study also provides an explanation to the enhanced NIR luminescence from Au nanodots (1.8 nm) via energy transfer from surface-bound fluorophores,[30] as we can see the red shift in the HOMO−LUMO gap of Au_{32} upon interaction with Trp in Figure 5 and Table 1.

3.3.3. Nature of Hybridization. The aromatic organic molecules are reported to show signatures of weak chemisorption at the gold surface, producing bonding- and antibonding-like hybrid orbitals below and above the middle of the metal d band as interpreted by the Newns−Anderson model (Figure 6f).[31] The model says that the metal d electron band interacts with the highest occupied electron level of the interacting atom and produces bonding and antibonding levels. Because the chemisorption is weak, the signatures for these levels are also expected to be weak. Thus, the nature of hybridization at the interacting interface of Trp−Au_{32} isomers is determined in detail from the computed projected density of states (PDOS).

dx.doi.org/10.1021/jp2070437 |J. Phys. Chem. C 2011, 115, 22818–22826

Figure 6 represents projected density of states (PDOS) centered on atoms involved in hybridization during Trp−Au_{32} conjugate formation compared to their native state. Figure 6a shows PDOS of native Au d electrons before conjugation, showing strong peaks in the −6 to −2 eV energy range and is apparently localized. Figure 6b shows the PDOS of p orbitals on native Trp atoms participating in the hybridization. The PDOS of carbon atoms in the indole ring are summed and presented together as the indole C, while the indole nitrogen N1 is shown separately. The structure of Trp with marked atom numbers is already shown in Figure 1b. The indole carbon atoms show sharp peaks due to presence of the delocalized π electron cloud from the aromatic ring. The nitrogen atom N1 is also a part of this aromatic π electron system and therefore found to follow the same trend observed in the indole C spectrum but with less intensity (Figure 6b). There is a strong peak noted around −1.2 eV and is attributed to the lone pair of nitrogen atom N2 of amine group in Trp. The oxygen O1 also appears with a strong peak around −3.5 eV related to its lone pairs. The oxygen atom O2 appears with two strong peaks around −3.5 and −2 eV related to its lone pair and carbonyl π electrons, respectively.

Figure 6c represents the PDOS of hybridizing atoms of the Trp−Au_{32} conjugate at the COOH site. Following the Newns−Anderson model, the energy range of −8 to −4 eV is assigned to the bonding region, and −2 to 0 eV is assigned to the antibonding region. The peaks corresponding to Au, oxygen O1 and O2, and indole C and N1 are modified compared to those of the initial spectrum in Figure 6b and confirm their participation in hybridization and contribution to bonding and antibonding orbitals. Figure 6d represents PDOS of the Trp−Au_{32} conjugate for the indole interaction site showing the participation of Au, C2, and indole C and N1 in hybridization and the formation of bonding and antibonding peaks in a range of −8 to −4 eV and −2 to 0 eV, respectively. Figure 6e shows PDOS of hybridizing atoms of the Trp−Au_{32} conjugate during NH_2 site interaction. Note from the figure that the lone pairs of N2 and O2 are largely modified, which confirms that Trp is interacting mainly through these atoms. O1 also seems to participate in this interaction, as its orbital signatures are modified. The antibonding region of the hybridizing system in all three interacting sites is actually crossed by the Fermi level; therefore, the region is found to be less populated. The presence of an underlying broad metal s band affects the nature of the hybrid bonding and antibonding orbitals and generates spread peaks rather than single localized peaks.

PDOS plots of Trp−Au isomers clearly demonstrate that the peak corresponding to the LUMO (∼1 eV) of the isomer is mainly centered at interacting Au atoms, though the higher excited levels show mixed Au−Trp character as evident by molecular orbital (Figure 4) and DOS analysis (Figure 5).

Small Au nanoparticles (size ≈1 nm) have been found to exhibit size-tunable luminescence properties,[32] and their luminescence efficiency is said to be increased by their interaction with electron-rich groups of the interacting fluorophore.[33] The Trp−Au_{32} system could potentially be used to study such applications, as we have seen discrete electronic states and the HOMO−LUMO gap in a Au_{32} cage together with the energy transfer pathway from excited states of Trp to Au. The synthetic reality of fullerenic Au_{32} will open new avenues for biological labels, energy transfer pairs, and other light-emitting sources in nanoscale electronics.

The Trp−Au nanoparticle interactions have important implications in various fields of research, as the interaction is currently being used for electroanalytical, SERS, and fluorescence sensing studies.[34,35] A recent experimental study has shown that Trp at the surface of Au nanoparticles is capable of producing strong SERS signals which were then used for detecting toxic mercury in trace amounts.[34] A Au nanoparticle-modified electrode was shown to improve the adsorption of Trp on the nanointerface and amplified the current response.[35] There are various studies utilizing fluorophore-conjugated Au nanoparticles for diagnosing/detecting biomolecules, cancer cells, bacteria, etc., using fluorescence sensing techniques.[36−38] During protein−nanoparticle interactions, as discussed earlier, Trp−nanoparticle interaction is an essential measure for determining protein structure and stability.[10,11] Note that the spatial position of Trp contributes to the protein tertiary structure. Our results predict that the indole group has strong affinity for Au (nonspecific π interaction) that may lead to disruption of helical structure, thereby resulting in protein aggregation, as shown by a recent study.[39]

4. CONCLUSION

First-principles calculations based on DFT are performed on Trp, Au_{32}, and Trp−Au_{32} to study the details of the nature of the interaction between tryptophan and gold. We find that the preference for binding that involves both carboxyl and indole functional groups, yielding the mixed salt-bridge and charge solvation structure, to be energetically more favorable and mediated by stronger-than-expected π interactions offered by the indole group. The present study does support the experimental finding of a ground-state Trp−Au complex formation. However, the present study depicts π interactions along with small ionic interactions instead of van der Waals interactions between Trp and Au nanoparticles. The hybridization during formation of stable the Trp−Au complex is anticipated to modify the nature of Trp's molecular orbitals by introducing hybrid states associated with Au as low-lying excited states. PDOS analysis suggests that these hybrid orbitals, produced by the coupling of a narrow Au d band with Trp atomic orbitals, have mixed metal−molecule character and are delocalized at the interface. The nonradiative energy transfer to these states is likely to cause the experimentally observed fluorescence quenching in Trp.[5,10,11]

AUTHOR INFORMATION

Corresponding Author

*E-mail: joship@ nplindia.org (P.J.); pandey@mtu.edu (R.P.).

ACKNOWLEDGMENT

We acknowledge the support from the Henry M. Jackson Foundation for the Advancement of Military Medicine, Inc. (611-243-2AFWP-00-104583). P.J. and V.S. thank Saikat Mukhopadhyay, Xiaoliang Zhong, and Sankar Gowtham for their help and also acknowledge the support received during their stay at Michigan Technological University.

REFERENCES

(1) Zhang, L.; Gu, F. X.; Chan, J. M.; Wang, A. Z.; Langer, R. S.; Farokhzad, O. C. *Clin. Pharmacol. Ther.* **2008**, *83*, 761–769.

(2) Chen, P. C.; Mwakwari, S. C.; Oyelere, A. K. *Nanotechnol., Sci. Appl.* **2008**, *1*, 45–66.

(3) De, M.; You, C. C.; Srivastava, S.; Rotello, V. M. *J. Am. Chem. Soc.* **2007**, *129*, 10747–10753.
(4) Lynch, I.; Dawson, K. A. *Nanotoday* **2008**, *3*, 40–47.
(5) Lacerda, S. H. D. P.; Park, J. J.; Meuse, C.; Pristinski, D.; Becker, M. L.; Karim, A.; Douglas, J. F. *ACS Nano* **2010**, *4*, 365–379.
(6) Brewer, S. H.; Glomm, W. R.; Johnson, M. C.; Knag, M. K.; Franzen, S. *Langmuir* **2005**, *21*, 9303–9307.
(7) Du, H.; Fuh, R. A.; Li, J.; Corkan, A.; Lindsey, J. S. *Photochem. Photobiol.* **1998**, *68*, 141–142.
(8) Vivian, J. T.; Callis, P. R. *Biophys. J.* **2001**, *80*, 2093–2109.
(9) Lindman, S.; Lynch, I.; Thulin, E.; Nilsson, H.; Dawson, K. A.; Linse, S. *Nano Lett.* **2007**, *7*, 914–920.
(10) Joshi, P.; Chakraborty, S.; Dey, S.; Shanker, V.; Ansari, Z. A.; Singh, S. P.; Chakrabarti, P. *J. Colloid Interface Sci.* **2011**, *355*, 402–409.
(11) Chakraborty, S.; Joshi, P.; Shanker, V.; Ansari, Z. A.; Singh, S. P.; Chakrabarti, P. *Langmuir* **2011**, *27*, 7722–7731.
(12) Selvakannan, P. R.; Mandal, S.; Phadtare, S.; Gole, A.; Pasricha, R.; Adyanthaya, S. D.; Sastry, M. *J. Colloid Interface Sci.* **2004**, *269*, 97–102.
(13) Si, S.; Mandal, T. K. *Chem.—Eur. J.* **2007**, *13*, 3160–3168.
(14) Kroto, H. W.; Heath, J. R.; Brian, S. C. O.; Curl, R. F.; Smalley, R. E. *Nature* **1985**, *318*, 162–163.
(15) Yin, W. J.; Gu, X.; Gong, X. G. *Solid State Commun.* **2008**, *147*, 323–326.
(16) Johansson, M. P.; Sundholm, D.; Vaara, J. *Angew. Chem., Int. Ed.* **2004**, *43*, 2678–2681.
(17) Joshi, P.; Shewale, V.; Pandey, R.; Shanker, V.; Hussain, S.; Karna, S. P. *Phys. Chem. Chem. Phys.* **2011**, *13*, 476–479.
(18) Martinez, E. V.; Labbe, A. T. *J. Comput. Chem.* **2010**, *31*, 2642–2649.
(19) Soler, J. M.; Artacho, E.; Gale, J. D.; García, A.; Junquera, J.; Ordejón, P.; Sánchez-Portal, D. *J. Phys.: Condens. Matter* **2002**, *14*, 2745–2779.
(20) Perdew, J. P.; Burke, K.; Ernzerhof, M. *Phys. Rev. Lett.* **1996**, *77*, 3865–3868.
(21) Troullier, N.; Martins, J. L. *Phys. Rev. B* **1991**, *43*, 1993–2006.
(22) Sánchez-Portal, D.; Artacho, E.; Soler, J. M. *J. Phys.: Condens. Matter* **1996**, *8*, 3859–3880.
(23) Gu, X.; Ji, M.; Wei, S. H.; Gong, X. G. *Phys. Rev. B* **2004**, *70*, 205401–5.
(24) Crespo, A.; Turjanski, A. G.; Estrin, D. A. *Chem. Phys. Lett.* **2002**, *365*, 15–21.
(25) The "salt-bridge" and "charge-solvent structure" are used to represent corresponding bonding sites following the nomenclature used in protein chemistry.
(26) Iori, F.; Felice, R. D.; Molinari, E.; Corni, S. *J. Comput. Chem.* **2009**, *30*, 1465–1476.
(27) Crespilho, F. N.; Lima, F. C. A.; Da-Silva, A. B. F.; Oliveira, O. N., Jr.; Zucolotto, V. *Chem. Phys. Lett.* **2009**, *469*, 186–190.
(28) Naka, K.; Itoh, H.; Tampo, Y.; Chujo, Y. *Langmuir* **2003**, *19*, 5546–5549.
(29) Iosin, M.; Baldeck, P.; Astilean, S. *J. Nanopart. Res.* **2010**, *12*, 2843–2849.
(30) Montalti, M.; Zaccheroni, N.; Prodi, L.; Reilly, N. O.; James, S. L. *J. Am. Chem. Soc.* **2007**, *129*, 2418–2419.
(31) Iori, F.; Corni, S.; Felice, R. D. *J. Phys. Chem. C* **2008**, *112*, 13540–13545.
(32) Zheng, J.; Zhang, C.; Dickson, R. M. *Phys. Rev. Lett.* **2004**, *93*, 077402.
(33) Wu, Z.; Jin, R. *Nano Lett.* **2010**, *10*, 2568–2573.
(34) Senapati, T.; Senapati, D.; Singh, A. K.; Fan, Z.; Kanchanapally, R.; Ray, P. C. *Chem. Commun.* **2011**, *47*, 10326–10328.
(35) Li, C.; Ya, Y.; Zhan, G. *Colloids Surf., B* **2010**, *76*, 340–345.
(36) Kato, N.; Caruso, F. *J. Phys. Chem. B* **2005**, *109*, 19604–612.
(37) Dubertret, B.; Calame, M.; Libchaber, A. J. *Nat. Biotechnol.* **2001**, *19*, 365–370.
(38) Wang, J.; Achilefu, S.; Nantz, M.; Kang, K. A. *Anal. Chim. Acta* **2011**, *695*, 96–104.
(39) Zhang, D.; Neumann, O.; Wang, H.; Yuwono, V. M.; Barhoumi, A.; Perham, M.; Hartgerink, J. D.; Stafshede, P. W.; Halas, N. J. *Nano Lett.* **2009**, *9*, 666–671.